Geomorphic Response of the Solani River Basin to Neotectonics: A Study from the Western Himalayan Foothills, India

Narendra K. Patel and Pitambar Pati

Abstract This study investigates the influence of neotectonics on the Solani River basin, using morphometric parameters, seismic signatures, and field-based study of unpaired river terraces. Morphometric parameters such as linear, areal, relief parameters, slope, aspect, stream-length (SL) index, and longitudinal river profile (LRP) suggest that the neotectonic activity triggered by the Himalayan tectonics affect the Solani River basin. Local convexity in the LRP indicates differential uplift along the associated faults. However, minor variation in knick points in LRP has been interpreted as rapid erosion due to unconsolidated to semi-consolidated nature of the sediments. The SL index of the Solani River ranges from 29.4 to 5233.2. The SL values along the river length indicates anomalies around the active fault zones. Mountain front sinuosity (S_{mf}) adjacent to the river basin ranges from 1.04 to 1.13, suggesting tectonically active nature of the region. Unpaired terraces reported at Roorkee and Toda-Kalyanpur at the right bank of the river are evidence of neotectonics. Three unpaired terraces reported at Roorkee, have riser-height of 1, 1.5, and 3 m and tread-width of 50, 40, and 70 m. While the riser and tread could not be measured at Toda-Kalyanpur due to their deformed nature. These E-W aligned terraces present 1.5 km south of the present river course dated back to 2.5 Ka (T_1) and 1.6 Ka (T_2). These terraces were formed due to the river shifting in response to the uplift of the river basin along with the Ganga plain. The upliftment rate along the Himalaya in the area shows a good coherency with few of the morphotectonic signatures of the basin. Other morphometric parameters such as hypsometry, asymmetry, valley width height ratio, did not yield supporting result, probably due to the DEM error and the unconsolidated nature of the sediments.

Keywords Solani River · Terraces · Neotectonics · Himalaya

N. K. Patel · P. Pati (✉)
Department of Earth Sciences, Indian Institute of Technology, Roorkee, Uttarakhand, India
e-mail: pitambar.pati@es.iitr.ac.in

N. K. Patel
e-mail: npatel@es.iitr.ac.in

H. N. Bhattacharya et al. (eds.), *Himalayan Neotectonics and Channel Evolution*,
Society of Earth Scientists Series, https://doi.org/10.1007/978-3-030-95435-2_4

1 Introduction

Landscape geomorphology epitomizes the balance between processes that produce and destroy topographic relief by uplifting and erosion (D'Arcy and Whittaker 2014). The landform evolution mechanism is regulated by various processes, such as lithology, tectonics, and climate change (Solanki et al. 2020). In high-level terrain, active tectonics during the recent geological period can be reflected by river incisions and sediment yields; diversion of channels, the formation of hanging tributaries and so on (Bull and McFadden 1977; Molin and Fubelli 2005; Kale and Shejwalkar 2008; Pati et al. 2018; Das 2020). However, alluvial plains like the Ganga plain respond to the neotectonics by abandoned river terraces, forming terminal fans, change in soil properties, and morphometric variations of the present and paleochannels. Morphometric analysis has widely been used to investigate the relationship between landform geometry and active faults (Kale and Shejwalkar 2008; Singh and Tandon 2008; Raj 2012; Pati et al. 2018; Gailleton et al. 2019; Das 2020). Quantitative landscape measurements may provide important information on geomorphic evolution and the degree of tectonic activity during recent geological times. Geomorphic indices are highly convenient tools for understanding active tectonics as these indices provide insights into particular sites that are rapidly adapting to variable tectonic deformation. The morphotectonic and field-based studies are widely used to locate undergoing tectonic deformation (Azor et al. 2002; Kirby and Whipple 2012; Han et al. 2017; Moodie et al. 2018; Pati et al. 2019; Patel et al. 2020).

The Solani, a tributary of the river Ganga has experienced frequent seismic activity with moderate-size earthquakes, epicentered around 10 km depth. Several studies have been performed to understand geology, stratigraphy, earthquake recurrence, and GPS measurements in the area (Jade 2004; Bhosle et al. 2008; 2009; Patel et al. 2020). The scale and methodology used in the earlier studies are highly generalized to apprehend the tectonic deformation of the area. However, a geomorphic evaluation supporting to the ongoing tectonic uplift is lacking in this area. Besides, any response to the neotectonic activity of the Himalayan segment can be studied along the respective foothill segments and their river systems. This study investigates the impact of the neotectonic activity on the Solani River basin using morphometric analysis, OSL chronology of alluvial terraces, and seismicity.

2 Study Area

2.1 Location

The study area lies between latitude 29–31°N and longitude 77–79°E. Politically it partly falls in Uttarakhand and Uttar Pradesh state of India. Thus, its northern extent is up to the Himalaya and southern extent is up Bijnor Uttar Pradesh. The Solani River is a tributary of the Ganga River, which originates from the Himalayan foothills

(Fig. 1). This monsoon-fed river has a catchment area of ~2009 km^2. It's ~150 km course passes through the Himalayan piedmont, consisting of boulders, pebbles, and

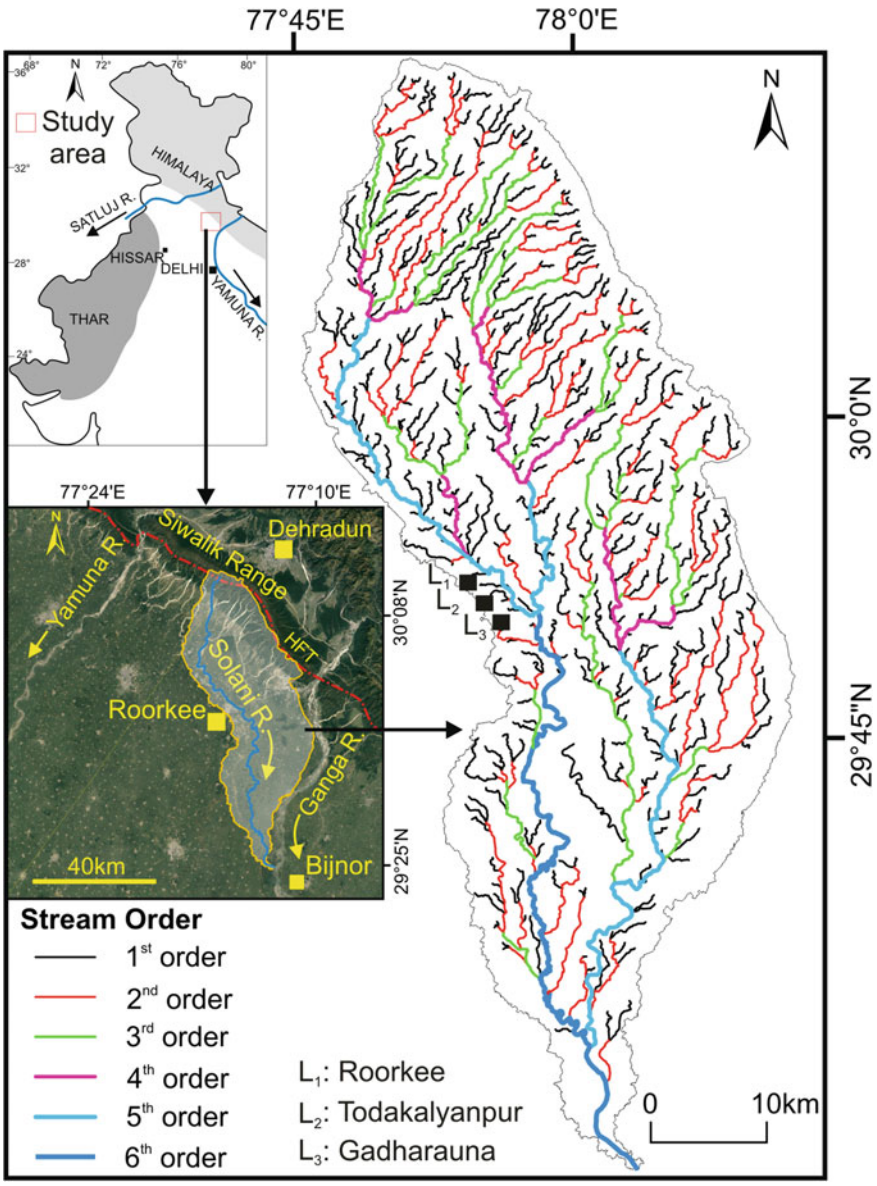

Fig. 1 Drainage map of the Solani River basin showing different orders of streams. The inset map shows the location of the study area

massive sandstones of Mio-Pliocene age and sandy to loamy Quaternary soils of the Ganga plain, until meeting the Ganga River.

2.2 Geology

The Solani River basin is a part of the western Ganga plain and lies in the Yamuna-Ganga interfluve (Fig. 2). The Solani River originates from the Himalaya foothills at Mohand. This incised river flows through a longitudinal fault (Solani fault), where the lower order tributaries follow less distance, and the trunk river continues further south and merges with the Ganga River near Bijnor of Uttar Pradesh. The river basin is restricted by the Ganga River in the east, the Yamuna River in the west, and the Siwalik in the north. Seismically active, the Mahendragarh-Dehradun Fault (MDF) following the Delhi-Haridwar ridge (Patel et al. 2020), passes along the western boundary of the basin (Fig. 3). Except the steep slope along the northern foothill piedmonts, running along the Siwalik's foothills, the river basin lacks any topographic prominence. The piedmont in the northern end is a narrow (10–25 km vast), elongated landscape, drained by several parallel to sub-parallel ephemeral streams. The piedmont is composed of gravel, sand, and clays, whereas the abundance of gravels decreases significantly from north to south. The river basin experiences semi-arid to sub-humid climate where annual precipitation varies from 500 to 1200 mm, out of which 80–85% is received between July and September (Kumar et al. 1996).

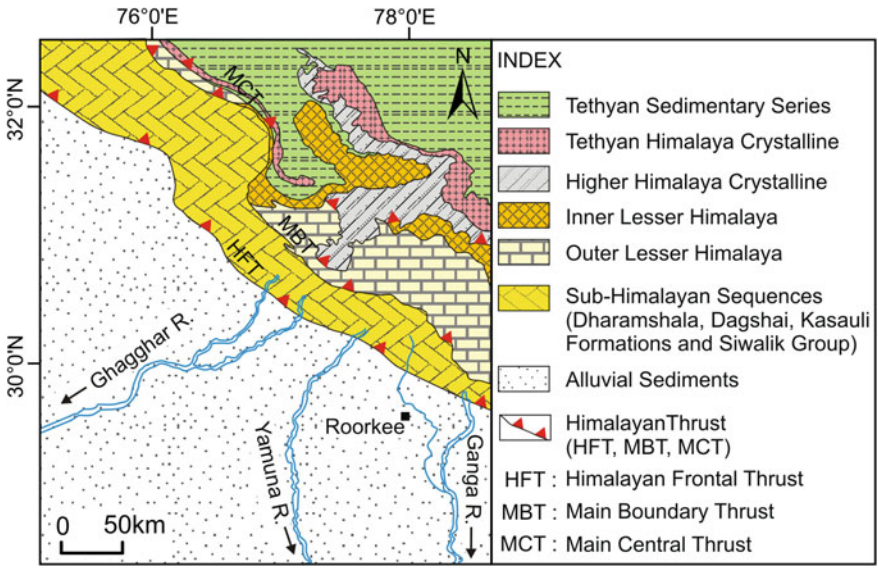

Fig. 2 Simplified geological map of NW Himalaya (modified after Singh et al. 2016)

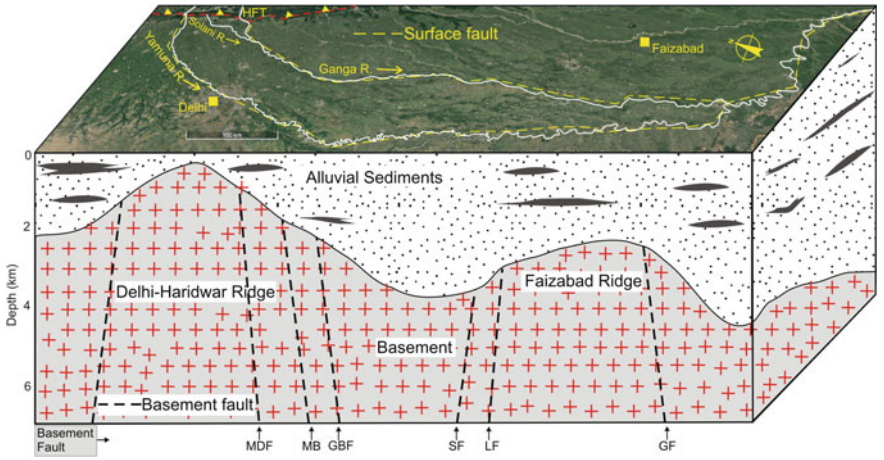

Fig. 3 Schematic diagram showing the basement configuration of the western Ganga plain. The Dehli–Haridwar ridge passes through the western boundary of the Solani River basin (modified after Gahalaut and Kundu 2012; MDF: Mahendragarh-Dehradun Fault, GBF: Great Boundary Fault, LF: Lucknow Fault, MF: Moradabad Fault, SF: Saharanpur Fault, GF: Gorakhpur Fault)

3 Materials and Methodology

Methodology followed in this study includes morphometric analysis, field study, and seismic data analysis.

3.1 Morphometric Analysis

We used ALOS data of 12.5 m resolution to evaluate the morphotectonics of the Solani River basin (Fig. 4). The datasets were validated using the Survey of India (SOI) topographic maps (1:50,000 scale) and Google Earth image. For the morphostructural analysis, the datasets were processed in ArcGIS 10.8 software on WGS 1984 datum. Field studies were carried out to validate the observations from the remote sensing based studies.

3.1.1 Bifurcation Ratio (R_b)

R_b is defined as the ratio of the number of streams in any given order to the number of streams in the next higher-order in the basin (Schumm 1956). It is a significant parameter that denotes the basin's water-carrying ability and related flood potential (Mahala 2020). A higher R_b value indicates a steep slope with impermeable or less permeable lithology, and a lower R_b value indicates the geological heterogeneity,

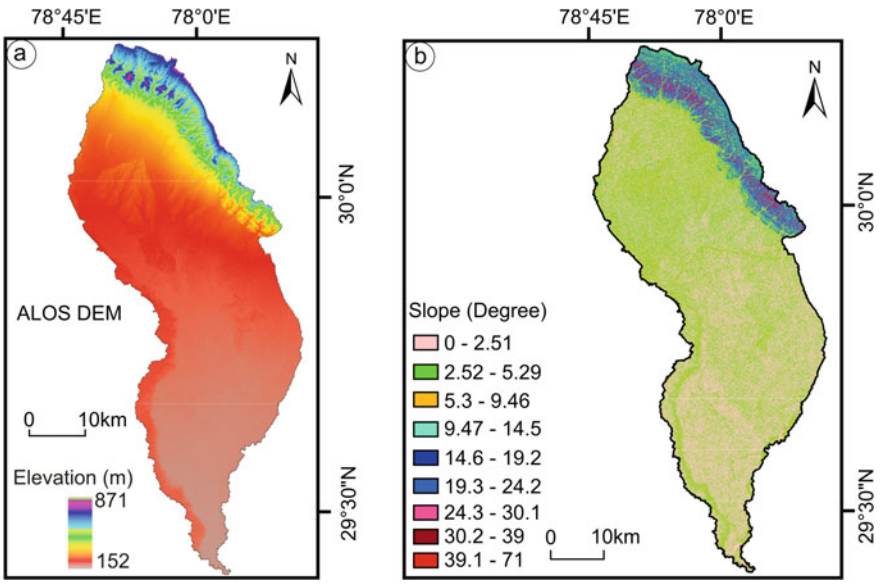

Fig. 4 **a** ALOS DEM of the Solani River basin showing topographic perception, **b** Slope map

higher permeable rocks with less structural control (Hajam et al. 2013). The R_b varies from 2.33 to 4.36, with a mean R_b of 3.46 for the Solani River basin (Table 1). This indicates that the basin falls under the normal category (Pandey and Das 2016). The high bifurcation ratio is found between 1st (4.36) and 2nd (4.04) order, and streams up to the 2nd order flow through strongly dissected and steep gradient of the piedmont area.

3.1.2 *Stream-Length Ratio (R_L)*

R_L is the ratio of the average length of the stream to one order to the next lower order (Horton 1945). It is an essential link between the discharge of the surface flow and the erosion of the basin. R_L for the Solani basin varies from 0.68 to 3.77, with an average R_L of 1.85 (Table 1). Higher values observed in the ratio of 1st and 2nd (1.95), 2nd and 3rd (1.77), and 3rd and 4th (3.37), which are strongly dependent on topography and slope, and in turn are controlled by the tectonic activity.

3.1.3 Elongation Ratio (Re)

Re is the ratio between the diameter of the circle of the same area as the drainage basin and the maximum length of the basin (Schumm 1956). It is believed that the elongated shapes of the basins are due to the guiding effect of thrusting and faulting

Table 1 Different geomorphic parameters studied for the Solani River basin

Basin parameters		
Basic parameter	Basin area	2009.27 km^2
	Basin perimeter	318.14 km
Linear parameters		
Number of streams	Number of first order streams (N1)	440
	Number of second order streams (N2)	447
	Number of third order streams (N3)	25
	Number of fourth order streams (N4)	7
	Number of fifth order streams (N5)	3
	Number of sixth order streams (N6)	1
	Total number of streams	577
Stream length (Lu)	Total length of first order streams (LT1)	870.83 km
	Total length of second order streams (LT2)	447 km
	Total length of third order streams (LT3)	252.38 km
	Total length of fourth order streams (LT4)	74.83 km
	Total length of fifth order streams (LT5)	109.62 km
	Total length of sixth order streams (LT6)	74.78 km
	Total length of the streams	1829.45 km
Mean stream length (Lsm)	Mean length of first order streams (L1)	1.98 km
	Mean length of second order streams (L2)	4.43 km
	Mean length of third order streams (L3)	10.10 km
	Mean length of fourth order streams (L4)	10.69 km
	Mean length of fifth order streams (L5)	36.54 km
	Mean length of sixth order streams (L6)	74.78 km
Bifurcation ratio (R_b)	1st/2nd order	4.36
	2nd/3rd order	4.04
	3rd/4th order	3.57
	4th/5th order	2.33
	5th/6th order	3.00
	Mean	3.46
Stream length ratio (R_L)	6th/5th	1.95
	5th/4th	1.77
	4th/3rd	3.37
	3rd/2nd	0.68
	2nd/1st	1.47
	Mean	1.85

(continued)

Table 1 (continued)

Basin parameters		
Basic parameter	Basin area	2009.27 km^2
	Basin perimeter	318.14 km
Rho coefficient (RHO)		0.53
Areal parameters	Drainage density (Dd)	0.91 km/km^2
	Stream frequency (Fs)	0.29
	Infiltration ratio	0.26
	Drainage texture (Dt)	1.81
	Form factor (Rf)	0.21
	Elongation ratio (Re)	0.52
	Circulatory ratio (Rc)	0.25
	Length of overland flow (Lo)	2.19
Relief aspect	Basin relief (Bh)	0.72 km
	Relief ratio (Rr)	0.0074
	Ruggedness number (Rn)	0.65
	Gradient ratio (Rg)	0.0054

in the basin (Zaidi 2011). The basins with lower Re values are susceptible to erosion (Sreedevi et al. 2009) because of moderate to high relief of the basin. The elongation ratio for the Solani River basin is 0.52 (Table1).

3.1.4 Longitudinal River Profile (LRP)

LRP is a very sensitive linear feature of tectonic deformation in the earth's crust (Holbrook and Schumm 1999; Whittaker et al. 2007; Viveen et al. 2012; Fekete and Vojtko 2013; Goren et al. 2014). Convex segments of LRP are called knickpoints or knickzones depending upon their length, which can be examined to determine their coincidence with tectonic disruptions (Molin and Fubelli 2005). Knickpoints in the LRP could serve as useful indicators of active structures along a river (Wobus et al. 2005). Fault movements will produce several small knick points in the channel profile (Zhang et al. 2011). In this study, LRP has been prepared for the Solani River (Fig. 5) using ALOS DEM. Avoiding the river confluences, the river shows multiple other local convexities along the LRP. Hence we interpret these knick points are related to tectonics.

3.1.5 Stream Length Gradient Index (SL Index)

Hack (1973) proposed a parameter known as the SL index to determine the geomorphological equilibrium. The SL index describes a stream network's morphology

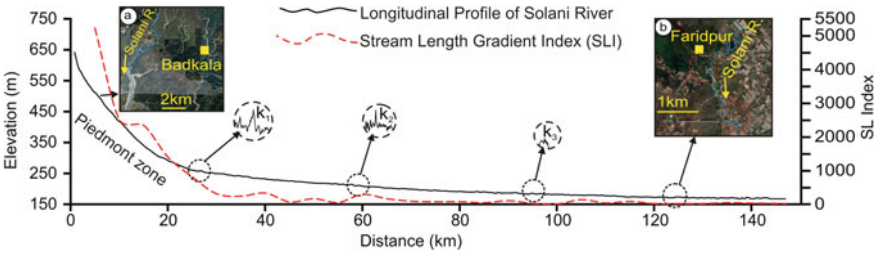

Fig. 5 Longitudinal river profiles and SL Index along the Solani River plotted together. **a** Google Earth image of the piedmont zone shows many first-order streams, **b** confluence of the river in the lower part of the basin shows minor knickpoints, k_1, k_2, and k_3 are the major knickpoints in the river profile

using the distribution of the topographic gradients along rivers (Font et al. 2010). It is sensitive to slope changes and allows to evaluate the tectonic activity, rock resistance, and topography (Keller and Pinter 2002) and is strictly related to the stream power (Moussi et al. 2018). A high SL index value may indicate if a particular region is experiencing tectonic activity or has any structural control. The SL index values of the Solani River range from 29.4 to 5233.2 (Fig. 5). The maximum value of SL index for the Solani River is 5233.2 (Piedmont region), and the minimum value is 29.4 (Plain region).

3.1.6 Mountain-Front Sinuosity Index (S_{mf})

Mountain-front sinuosity has been applied to study mountain front tectonics by several researchers (Ramírez-Herrera 1998; Frankel and Pazzaglia 2005; Azañón et al. 2012; Mahmood and Gloaguen 2012; Dar et al. 2013; Elias 2015; Topal et al. 2016; Bhakuni et al. 2017; Giaconia et al. 2012) in different parts of the globe (Bull and McFadden 1977; Keller and Pinter 2002; Silva et al. 2003; Pérez-Peña et al. 2010; Giaconia et al. 2012). Along the active mountain fronts, uplift prevails over erosional processes, yielding straight fronts with low values of S_{mf}. Along less active fronts, erosional processes generate irregular or sinuous fronts with high values of S_{mf} (Azañón et al. 2012; Topal et al. 2016). Bull and McFadden (1977) defined mountain front sinuosity (S_{mf}) as an index that reflects the balance between erosional forces and tectonic processes that control the embayment of the mountain front to make it linear.

Mountain-front sinuosity was defined by Bull (1977) as $S_{mf} = L_{mf} / L_s$.

Where, S_{mf}: mountain front sinuosity.

L_{mf}: length of the mountain front along the foot of the mountain along the pronounced break in slope.

L_s: length of the mountain front measured along a straight line.

S_{mf} reflects the balance between erosion forces that tend to cut embayment into a mountain front and tectonic forces that tend to produce a straight mountain front

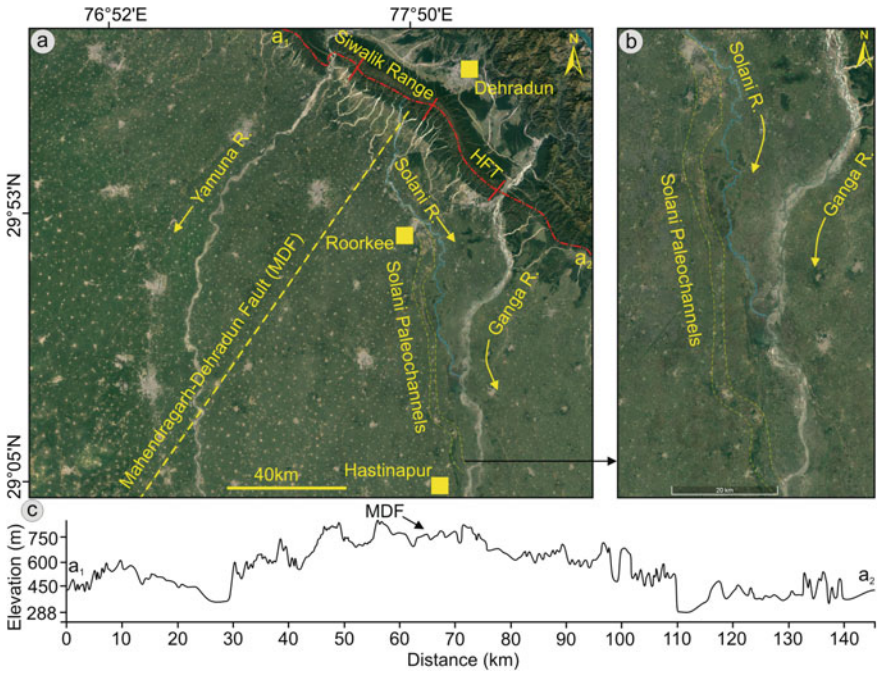

Fig. 6 **a** Piedmont zone showing many first and second-order streams, **b** major paleochannels in the area, **c** profile along the HFT shows upliftment

coincident with an active range-bounding fault (Verrios et al. 2004). S_{mf} of highly active mountain fronts generally ranges from 1.0 to 1.5, that of moderately active fronts ranges from 1.5 to 3, and that of inactive fronts ranges from 3 to more than 10 (Elias 2015). Some other studies have proposed that the values of the S_{mf} index lower than 1.4 are indicative of tectonically active fronts (Silva et al. 2003). It is possible to understand tectonic activity and Quaternary landscape evolution through the application of such geomorphic analyses. Young mountain fronts tend to have low values of S_{mf}, as they have not experienced significant range-front erosion and are responding to active tectonic uplift on a relatively steep fault, keeping it approximately straight (Topal et al. 2016). In the present study, the S_{mf} varies from 1.1 to 1.2, indicating the active nature of the region with pronounced uplift (Fig. 6).

3.2 Field Study

The Solani River basin was studied by detailed fieldwork. During the fieldwork, three unpaired terraces at Roorkee, and two unpaired terraces at Toda Kalyanpur have been studied (Figs. 7 and 8).

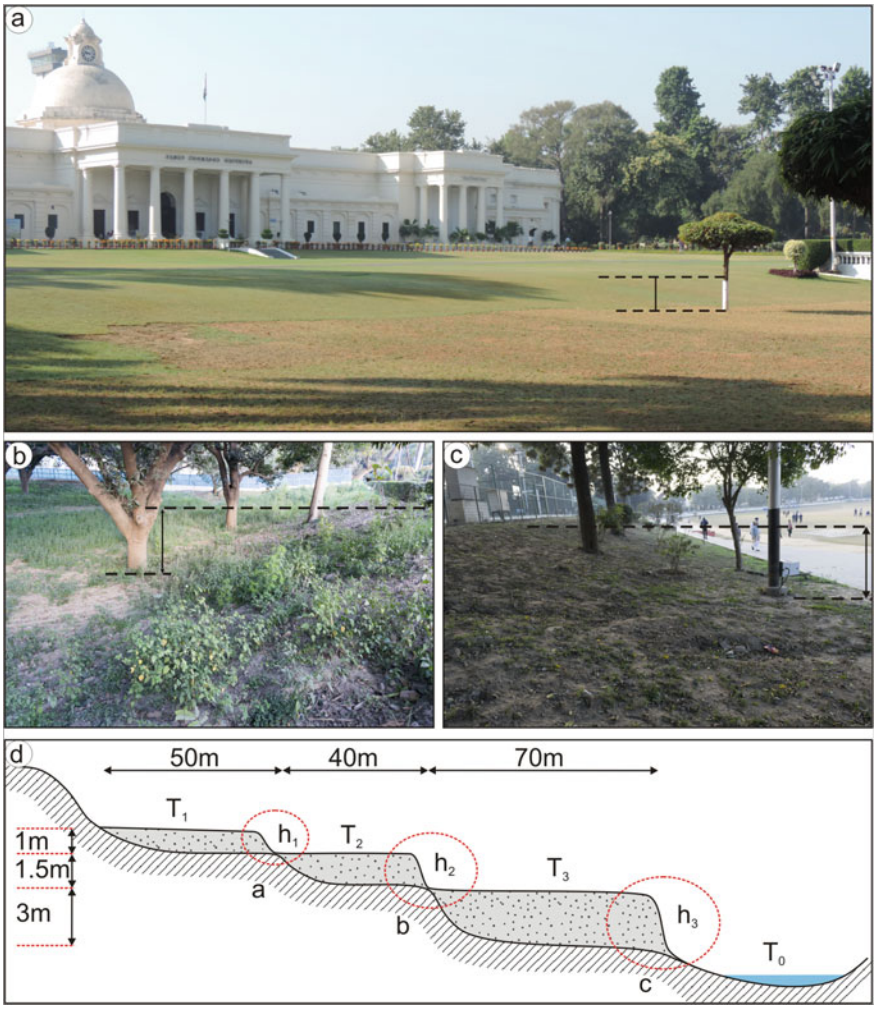

Fig. 7 **a–c** are the field photos of terraces, **d** schematic diagram of the Solani River terraces at Roorkee

3.3 Seismic Activity

Paleoseismology uses elements of tectonic geomorphology, sedimentology and stratigraphy to assess the position timing and displacement of past earthquakes (Kondo and Owen 2013). Recent technological advances including remote sensing, geodesy, fault trenching and computational dating have helped to accelerate knowledge and analysis of past earthquakes. Efficient seismic hazard mapping requires the creation of ground acceleration maps based on high resolution, accurate geomorphic and quaternary geological mapping. Geomorphology is the primary tool for

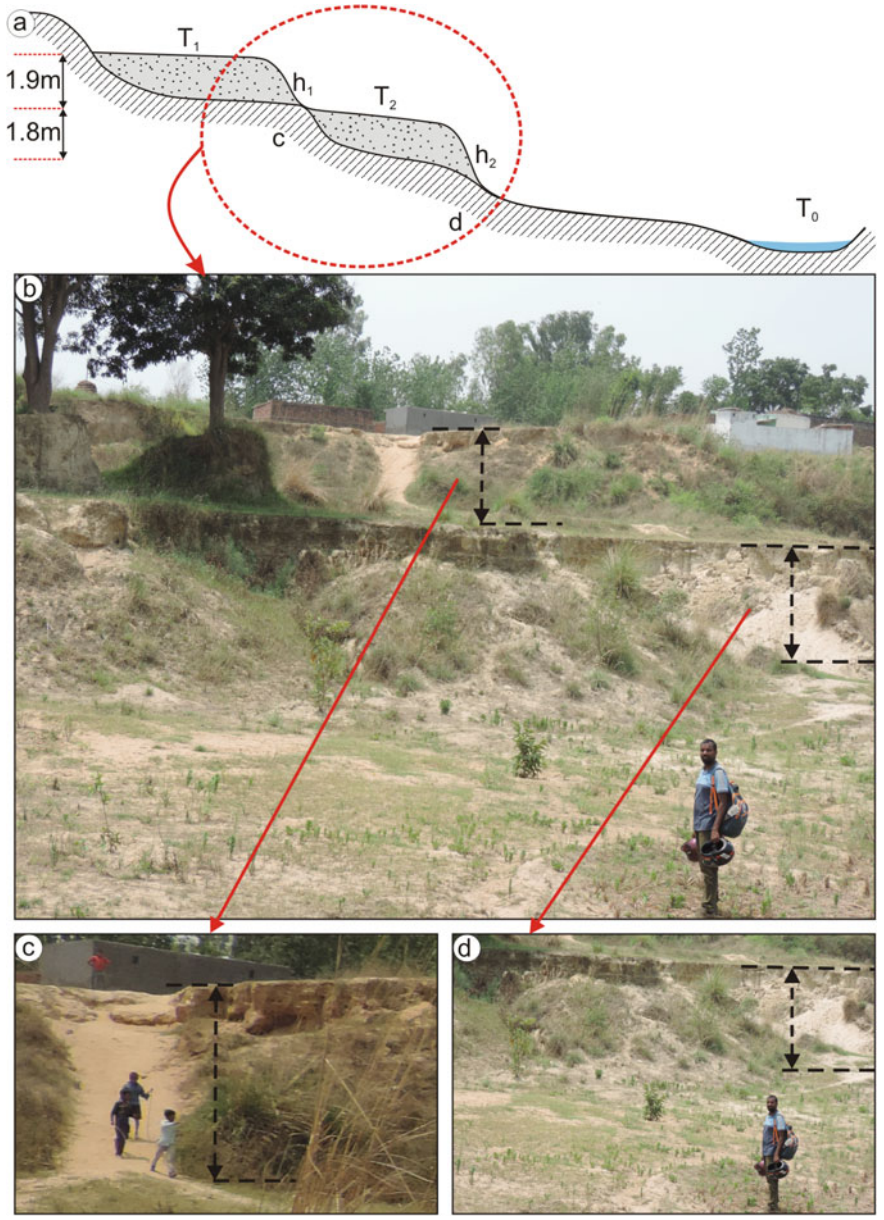

Fig. 8 **a** Schematic diagram of the Solani River terraces at Todakalyanpur, **b–d** are the field photos of the terraces

neotectonics, earthquake geology, paleoseismology studies and evaluation of seismic hazards. The geomorphology of active fault plays a dominant role in the collection of such data (Kondo and Owen 2013). Neotectonic activity in the present area of study has been well recorded by several seismic events in recent years (Fig. 9). These seismic events indicate active tectonics in the area.

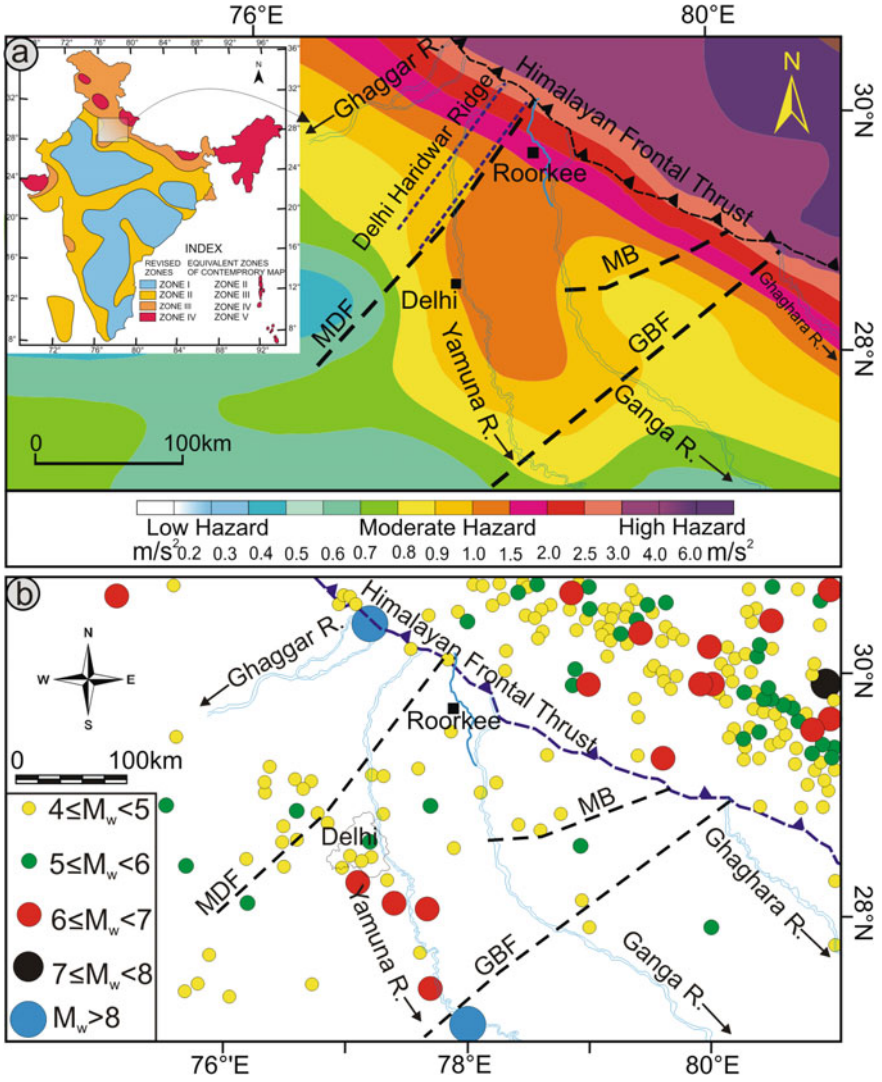

Fig. 9 Seismicity map of the western Ganga plain shows seismicity pattern in and around the Solani River basin. **a** Seismic Hazard map (data compiled from http://asc-india.org, inset shows seismic zone of India with the location of the study area), **b** Distribution of faults and seismic pattern (for abbreviations refer to Fig. 3, seismic data taken from Prabhu and Raghukanth 2015)

4 Neotectonic Movements and Channel Evolution

It is difficult to describe any parameter that would systematically isolate the tectonic effect on a river basin. However, the morphometric analysis of the Solani basin has provided evidence for the influence of neotectonics. Kumar et al. (1996) delineated many paleochannels on a regional scale, which shows the river's northeastward shift of channel. Modern channels also show meandering and northeastward shifting (Fig. 10). This long-term unidirectional shift may be due to tilting of the tectonic clock due to the ongoing NE-SW compression. LRP shows the local convexity corresponds the knickpoints and tributary junction. However, ignoring the confluences, all other local convexities are due to local structural perturbations. The SL index plotted along the LRP is showing a good correlation. The stream length gradient index and LRP coroborate each other, indicating neotectonic influence in the river basin.

Paleochannels in the area begin near to Roorkee and end near to Hastinapur (Fig. 10). The "folklore", as verbally stated by the natives, are are the Burhi (Old) Ganga channel (Kumar et al. 1996) (through depicted by the Aeolian ridges and without any significant channels, Fig. 11). The Hindu epic Mahabharat states that Hastinapur was the capital of the Kaurava-King Prikhsit, and he had to shift his

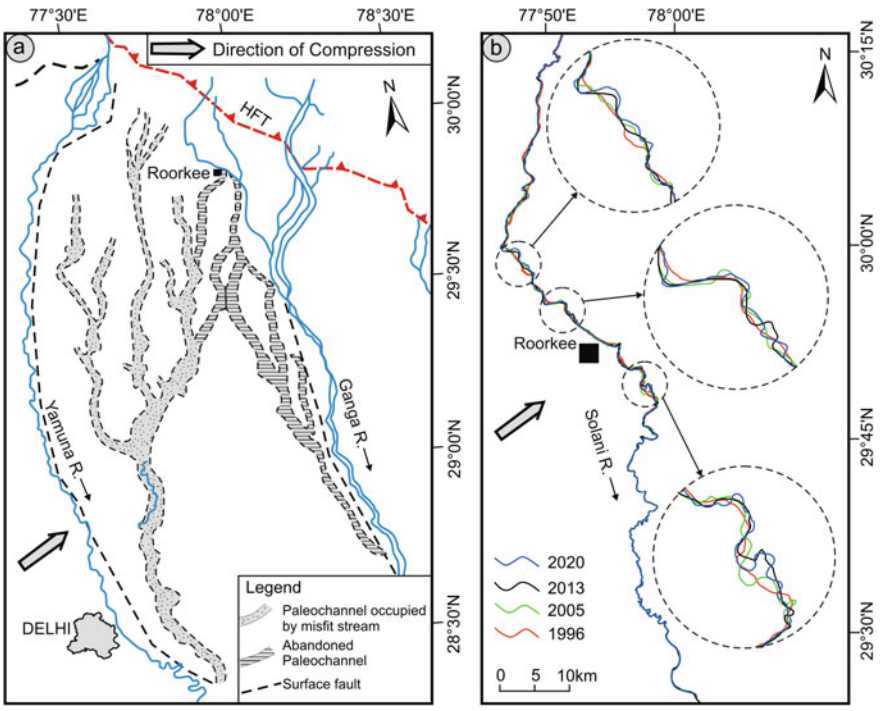

Fig. 10 **a** Mapping of paleochannels shows river shifting towards the east (modified after Kumar et al. 1996), **b** the migration of recent Solani channels

Fig. 11 Field photographs of the alluvial ridges in the Solani River deposits around Gadharauna

capital from Hastinapur due to floods in the Ganga (Thaper 1966). The Mahabharat Era is closely related to the Painted Gray Ware (PGW) culture, and the later dated back to 600–1000 B.C. (Lal 1954–55, 1981). The flooding time of Hastinapur was dated 800 B.C. (Thaper 1966). This suggests the Ganga River flowed on this upland region (about 15 m higher than the Ganga flood plain, where the present Ganga River flows) sometime before 600 B.C.

The Solani River basin records neotectonic activities in the Ganga plain along its course. Unpaired tectonic terraces at Roorkee and Toda Kalyanpur at the river's right bank are evidence of faulting and river shifting (Figs. 7 and 8). At Roorkee, three terraces have been identified, having riser of 1, 1.5, and 3 m height and tread of 50, 40, and 70 m width, respectively, while riser and tread cannot be measured at Toda-Kalyanpur due to the deformation. These terraces are about 2 km south from the present river course. Different generations of river terraces in the Ganga plain are generally distinguished by their respective degree of soil development. However, the presently studied terraces have no signature of soil development, indicating that they are very recently developed. These terraces were formed by upliftment of the Ganga plain due to compression along the Himalayan front and subsequent river shifting. The Ganga plain is tectonically active by its coupled nature with the Himalaya (Parkash et al. 2011). River courses in the Ganga plain are continuously shifting in one direction due to the area's compression and upliftment. The results allow in reconstructing the Holocene evolution of the river valley and correlating the processes that led to the terrace formation.

Four unpaired terraces (T_0–T_3), were recognized along the right bank of the Solani River (Vorha 1987). The T_3 lies 14–18 m above the present Solani River bed (T_0), Terrace T_3 and T_2 were dated using the Thermo Luminescence (TL) technique by Vhora (1987) and assigned ages 2500 and 1600 cal. B.P., respectively. The date for the T_3 terrace is the same order of magnitude, as indicated by the PGW culture. Unpaired tectonic terraces and the morphometric parameters suggest temporal activity of the Solani fault.

Unpaired terraces and different faults are indicative of the ongoing tectonic activity in the area. These terraces, composed of fluvial deposits, prominently stand above the modern river channel. Morphotectonic parameters indicate tectonic movements along the MDF, which is close to the Solani basin (Patel et al. 2020). Paleochannels of Solani River are linear in nature, associated with terraces, are indicative of migration of the river (Fig. 6b).

The Himalaya along with the Solani basin experience strong compressional stress (Zoback 1992). Due to the tectonic activity along the Solani, Yamuna, and Ganga faults, the upper Ganga-Yamuna block was raised, and the Ganga-Ramganga block was thrown down (Kumar et al. 1996, Fig. 12). This is clear evidence of the tectonic upliftment of the area. Since its origin, the Ganga plain has undergone numerous geomorphic changes due to tectonic activity (Mohindra et al. 1992). Finite element modelling of the Ganga plain by Parkash et al. (2000) indicates that SW compression (Fig. 12) develops longitudinal faults (parallel to sub-parallel with the Himalayan trend) and extensional transverse normal faults (an angle to the Himalayans trend). Using the Global Positioning System (GPS), Jade (2004) indicates the displacement of the Indian plate to the northwest. The above works support the mechanism for the creation of longitudinal and transverse faults in the Ganga plain studied by several researchers (Singh et al. 2006; Bhosle et al. 2007, 2008; Pati et al. 2018, 2019; Verma et al. 2017; Patel et al. 2020). The present study confirms the existence of active tectonics in the area and highlights its role in shaping the Solani River basin.

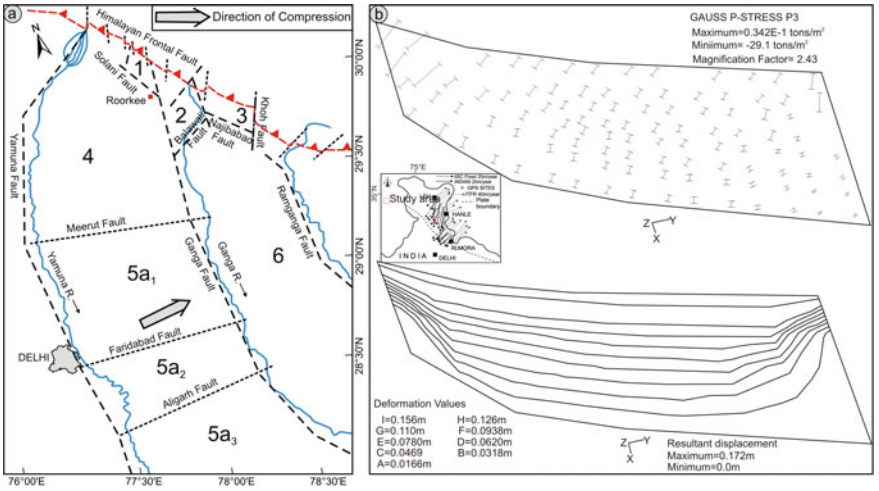

Fig. 12 **a** Surficial faults and tectonic blocks in the area. 1—Solani block, 2—Ganga Solani block, 3—Khoh block, 4—Upper Ganga-Yamuna block, $5a_1$—Modinagar subblock, $5a_2$—Khurja sub-block, $5a_3$—Etah sub-block, and 6—Ganga-Ramganga block (modified after Kumar et al. 1996), **b** Finite element model after Parkash et al. (2000) shows compression from SW develops longitudinal faults in the area. GPS movement was taken from Jade (2004) (Inset figure)

5 Conclusions

The tectono-geomorphic investigations of the Solani River basin was conducted in the western Ganga plain on the basis of ALOS DEM analysis. The morphometric analysis, seismic, and field-based study helps us to reach the following conclusions.

1. The Solani River basin is a sixth-order river basin with the dominance of lower-order streams.
2. The unpaired terraces at Roorkee and Toda Kalyanpur are evidence of neotectonics.
3. Seismicity and morphometric parameters indicate the river basin is tectonically influenced.
4. Tectonic influence in the Solani River basin is due to its position adjacent to a highly compressed zone of the Himalayan front, where significant upliftment has been recorded.

References

Azañón JM, Pérez-Peña JV, Giaconia F, Booth-Rea G, Martínez-Martínez JM, Rodríguez-Peces MJ (2012) Active tectonics in the central and eastern Betic Cordillera through morphotectonic

analysis: the case of Sierra Nevada and Sierra Alhamilla. J Iber Geol 38:225–238. https://doi.org/10.5209/rev_JIGE.2012.v38.n1.39214

Azor A, Keller EA, Yeats RS (2002) Geomorphic indicators of active fold growth: South Mountain-Oak Ridge anticline, Ventura basin, southern California. Bull Geol Soc Am 114:745–753. https://doi.org/10.1130/0016-7606(2002)114%3c0745:GIOAFG%3e2.0.CO;2

Bhakuni SS, Luirei K, Kothyari GC, Imsong W (2017) Transverse tectonic structural elements across Himalayan mountain front, eastern Arunachal Himalaya, India: implication of superposed landform development on analysis of neotectonics. Geomorphology 282:176–194. https://doi.org/10.1016/j.geomorph.2016.12.025

Bhosle B, Parkash B, Awasthi AK, Singh VN, Singh S (2007) Remote sensing-GIS and GPR studies of two active faults, Western Gangetic Plains, India. J Appl Geophys 61:155–164. https://doi.org/10.1016/j.jappgeo.2006.10.003

Bhosle B, Parkash B, Awasthi AK, Pati P (2009) Use of digital elevation models and drainage patterns for locating active faults in the Upper Gangetic Plain, India. Int J Remote Sens 30:673–691

Bhosle B, Parkash B, Awasthi AK, Singh S, Khan MSH (2008) Role of extensional tectonics and climatic changes in geomorphological, pedological and sedimentary evolution of the Western Gangetic Plain (Himalayan Foreland Basin), India. Himalayan Geol 29:1–24

Bull WB (1977) The alluvial-fan environment. Progr Phys Geogr: Earth Environ 1:222–270. https://doi.org/10.1177/030913337700100202

Bull WB, McFadden LD (1977) Tectonic geomorphology north and south of the Garlock fault, California. Geomorphol Arid Reg 115–138

Dar RA, Chandra R, Romshoo SA (2013) Morphotectonic and lithostratigraphic analysis of intermontane Karewa Basin of Kashmir Himalayas, India. J Mt Sci 10:1–15. https://doi.org/10.1007/s11629-013-2494-y

Das S (2020) Koyna-Warna Shallow seismic region, India: is there any geomorphic expression of active tectonics? J Geol Soc India 96:217–231. https://doi.org/10.1007/s12594-020-1541-x

D'Arcy M, Whittaker AC (2014) Geomorphic constraints on landscape sensitivity to climate in tectonically active areas. Geomorphology 204:366–381. https://doi.org/10.1016/j.geomorph.2013.08.019

Elias Z (2015) The neotectonic activity along the lower Khazir River by using SRTM image and geomorphic indices. Earth Sci 4:50. https://doi.org/10.11648/j.earth.20150401.15

Fekete K, Vojtko R (2013) Neotectonic activity of the Pravno fault in the area of the Ziar Mts. Acta Geologica Slovaca 5:117–127

Font M, Amorese D, Lagarde JL (2010) DEM and GIS analysis of the stream gradient index to evaluate effects of tectonics: the Normandy intraplate area (NW France). Geomorphology 119:172–180. https://doi.org/10.1016/j.geomorph.2010.03.017

Frankel KL, Pazzaglia FJ (2005) Tectonic geomorphology, drainage basin metrics, and active mountain fronts. Geogr Fis Din Quat 28:7–21

Gahalaut VK, Kundu B (2012) Possible influence of subducting ridges on the Himalayan arc and on the ruptures of great and major Himalayan earthquakes. Gondwana Res 21:1080–1088. https://doi.org/10.1016/J.GR.2011.07.021

Gailleton B, Mudd SM, Clubb FJ, Peifer D, Hurst MD (2019) A segmentation approach for the reproducible extraction and quantification of knickpoints from river long profiles. Earth Surf Dyn 7:211–230. https://doi.org/10.5194/esurf-7-211-2019

Giaconia F, Booth-Rea G, Martínez-Martínez JM, Azañón JM, Pérez-Peña JV, Pérez-Romero J, Villegas I (2012) Geomorphic evidence of active tectonics in the Sierra Alhamilla (eastern Betics, SE Spain). Geomorphology 145–146:90–106. https://doi.org/10.1016/j.geomorph.2011.12.043

Goren L, Fox M, Willett SD (2014) Tectonics from fluvial topography using formal linear inversion: theory and applications to the Inyo Mountains, California. J Geophys Res F: Earth Surf 119:1651–1681. https://doi.org/10.1002/2014JF003079

Hack JT (1973) Stream-profile analysis and stream-gradient index. J Res US Geol Surv 1:421–429

Hajam RA, Hamid A, Bhat S (2013) Application of morphometric analysis for geo-hydrological studies using geo-spatial technology—a case study of Vishav Drainage Basin. Hydrol Curr Res 4:1–12. https://doi.org/10.4172/2157-7587.1000157

Han Z, Xusheng LI, Wang N, Chen G, Wang X, Huayu LU (2017) Application of river longitudinal profile morphometrics to reveal the uplift of Lushan Mountain. Acta Geol Sin 91:1644–1652. https://doi.org/10.1111/1755-6724.13403

Holbrook J, Schumm SA (1999) Geomorphic and sedimentary response of rivers to tectonic deformation: a brief review and critique of a tool for recognizing subtle epeirogenic deformation in modern and ancient settings. Tectonophysics 305:287–306. https://doi.org/10.1016/S0040-1951(99)00011-6

Horton RE (1945) Erosional development of streams and their drainage basins, hydrographical approach to quantitative morphology. Geol Soc Am Bull 56:275–370. https://doi.org/10.1130/0016-7606(1945)56[275:EDOSAT]2.0.CO;2

Jade S (2004) Estimates of plate velocity and crustal deformation in the Indian subcontinent using GPS. Curr Sci 86:1143–1448

Kale VS, Shejwalkar N (2008) Uplift along the western margin of the Deccan Basalt Province: is there any geomorphometric evidence? J Earth Syst Sci 117:959–971. https://doi.org/10.1007/s12040-008-0081-3

Keller E, Pinter N (2002) Active tectonics: earthquakes, uplift and landscape. New Jersey

Kirby E, Whipple KX (2012) Expression of active tectonics in erosional landscapes. J Struct Geol 44:54–75

Kondo H, Owen LA (2013) 5.12 Paleoseismology. In: Shroder JF (ed) Treatise on geomorphology. Academic Press, Cambridge, pp 267–299

Kumar S, Parkash B, Manchanda ML, Singhvi AK, Srivastava P (1996) Holocene landform and soil evolution of the western gangetic plains: implications of neotectonics and climate. Zeitschrift Fur Geomorphologie, Supplementband 103:283–312

Lal BB (1954–55) Excavations at Hastinapur and other explorations in the Upper Ganga and Sutlej Basins. Ancient India 10–11:5–151

Lal BB (1981) The two Indians epics vis-à-vis Indian Archeology. Antiquity 55:27–34

Mahala A (2020) The significance of morphometric analysis to understand the hydrological and morphological characteristics in two different morpho-climatic settings. Appl Water Sci 10:1–16. https://doi.org/10.1007/s13201-019-1118-2

Mahmood SA, Gloaguen R (2012) Appraisal of active tectonics in Hindu Kush: Insights from DEM derived geomorphic indices and drainage analysis. Geosci Front 3:407–428. https://doi.org/10.1016/j.gsf.2011.12.002

Mohindra R, Parkash B, Prasad J (1992) Historical geomorphology and pedology of the Gandak Megafan, middle gangetic plains, India. Earth Surf Proc Land 17:643–662. https://doi.org/10.1002/esp.3290170702

Molin P, Fubelli G (2005) Morphometric evidence of the topographic growth of the central Apennines. Geogr Fis Din Quat 28:47–61

Moodie AJ, Pazzaglia FJ, Berti C (2018) Exogenic forcing and autogenic processes on continental divide location and mobility. Basin Res 30:344–369. https://doi.org/10.1111/bre.12256

Moussi A, Rebaï N, Chaieb A, Saâdi A (2018) GIS-based analysis of the stream length-gradient index for evaluating effects of active tectonics: a case study of Enfidha (North–East of Tunisia). Arab J Geosci 11:123

Pandey PK, Das SS (2016) Morphometric analysis of Usri River basin, Chhotanagpur Plateau, India, using remote sensing and GIS. Arab J Geosci 9:240. https://doi.org/10.1007/s12517-015-2287-4

Parkash B, Kumar S, Rao MS, Giri SC, Kumar CS, Gupta S, Srivastava P (2000) Holocene tectonic movements and stress field in the western Gangetic plains. Curr Sci 79:438–449

Parkash B, Rathor RS, Pati P, Jakhmola RP, Singh S (2011) Convergence rates along the Himalayan Frontal Thrust inferred from terraces at Chandidevi Temple Hill, Hardwar, Northwestern Himalaya. Curr Sci 100:1426–1432

Patel NK, Pati P, Verma AK, Dash C, Gupta A, Sharma V (2020) Seismicity around the Mahendragarh-Dehradun basement fault in the western Ganga plain, India: a neotectonic perspective. Int J Earth Sci 109:689–706. https://doi.org/10.1007/s00531-020-01826-8

Pati P, Acharya V, Verma AK, Patel NK, Jakhmola RP, Dash C, Sharma V, Gupta A, Parkash B, Awasthi AK (2018) Holocene tectono-geomorphic evolution of Haryana plains, Western Ganga plain, India. Arab J Geosci 11:361. https://doi.org/10.1007/s12517-018-3714-0

Pati P, Verma AK, Dash C, Patel NK, Gupta A, Sharma V, Jakhmola R, Parkash B, Awasthi AK, Saraf AK (2019) Influence of neotectonism on geomorphology and depositional architecture of the Gandak megafan, middle Ganga plain, India. Geomorphology 327:489–503. https://doi.org/10.1016/j.geomorph.2018.11.029

Prabhu M, Raghukanth STG (2015) Development of surface level probabilistic seismic hazard map of Himachal Pradesh. Advances in structural engineering: dynamics, vol 2. Springer India, New Delhi. https://doi.org/10.1007/978-81-322-2193-7_60

Pérez-Peña JV, Azor A, Azañón JM, Keller EA (2010) Active tectonics in the Sierra Nevada (Betic Cordillera, SE Spain): Insights from geomorphic indexes and drainage pattern analysis. Geomorphology 119:74–87. https://doi.org/10.1016/j.geomorph.2010.02.020

Raj R (2012) Active tectonics of NE Gujarat (India) by morphometric and morphostructural studies of Vatrak River basin. J Asian Earth Sci 50:66–78. https://doi.org/10.1016/j.jseaes.2012.01.010

Ramírez-Herrera MT (1998) Geomorphic assessment of active tectonics in the acambay graben, Mexican volcanic belt. Earth Surf Proc Land 23:317–332. https://doi.org/10.1002/(SICI)1096-9837(199804)23:4%3c317::AID-ESP845%3e3.0.CO;2-V

Schumm SA (1956) Evolution of drainage systems and slopes in badlands at Perth Amboy, New Jersey. Bull Geol Soc Am 67:597–646. https://doi.org/10.1130/0016-7606(1956)67[597:EODSAS]2.0.CO;2

Seismic Hazard Data (2020) http://asc-india.org/maps/hazard/haz-cdh.htm. Accessed 7 Sept 2020

Silva PG, Goy JL, Zazo C, Bardají T (2003) Faulth-generated mountain fronts in southeast Spain: geomorphologic assessment of tectonic and seismic activity. Geomorphology 50:203–225. https://doi.org/10.1016/S0169-555X(02)00215-5

Singh S, Parkash B, Rao MS, Arora M, Bhosle B (2006) Geomorphology, pedology and sedimentology of the Deoha/Ganga–Ghaghara Interfluve, Upper Gangetic Plains (Himalayan foreland basin)-extensional tectonic implications. Catena 67:183–203. https://doi.org/10.1016/j.catena.2006.03.013

Singh A, Paul D, Sinha R, Thomsen KJ, Gupta S (2016) Geochemistry of buried river sediments from Ghaggar Plains, NW India: Multi-proxy records of variations in provenance, paleoclimate, and paleovegetation patterns in the Late Quaternary. Palaeogeogr Palaeoclimatol Palaeoecol 449:85–100. https://doi.org/10.1016/j.palaeo.2016.02.012

Singh V, Tandon SK (2008) The Pinjaur dun (intermontane longitudinal valley) and associated active mountain fronts, NW Himalaya: Tectonic geomorphology and morphotectonic evolution. Geomorphology 102:376–394. https://doi.org/10.1016/j.geomorph.2008.04.008

Solanki T, Solanki PM, Makwana N, Prizomwala S, Kothyari GC (2020) Geomorphic response to neotectonic instability in the Deccan volcanic province, Shetrunji River, western India: insights from quantitative geomorphology. Quatern Int. https://doi.org/10.1016/j.quaint.2020.06.015

Sreedevi PD, Owais S, Khan HH, Ahmed S (2009) Morphometric analysis of a watershed of South India using SRTM data and GIS. J Geol Soc India 73:543–552. https://doi.org/10.1007/s12594-009-0038-4

Thapar R (1966) A history of India, vol I. Penguin Book Ltd., Middlesex, England

Topal S, Keller E, Bufe A, Koçyiğit A (2016) Tectonic geomorphology of a large normal fault: Akşehir fault, SW Turkey. Geomorphology 259:55–69

Verma AK, Pati P, Sharma V (2017) Soft sediment deformation associated with the East Patna Fault south of the Ganga River, northern India: influence of the Himalayan tectonics on the southern Ganga plain. J Asian Earth Sci 143:109–121. https://doi.org/10.1016/j.jseaes.2017.04.016

Verrios S, Zygouri V, Kokkalas S (2004) Morphotectonic analysis in the Eliki fault zone (Gulf of Corinth, Greece). Bull Geol Soc Greece 36:1706–1715

Vhora MS (1987) Thermoluminescence dating of fluvial terraces: a feasibility study. Unpublished M. Tech. disseration, University of Roorkee (Present IIT Roorkee)

Viveen W, van Balen RT, Schoorl JM, Veldkamp A, Temme AJAM, Vidal-Romani JR (2012) Assessment of recent tectonic activity on the NW Iberian Atlantic Margin by means of geomorphic indices and field studies of the Lower Miño River terraces. Tectonophysics 544–545:13–30. https://doi.org/10.1016/j.tecto.2012.03.029

Whittaker AC, Cowie PA, Attal M, Tucker GE, Roberts GP (2007) Bedrock channel adjustment to tectonic forcing: implications for predicting river incision rates. Geology 35:103–106. https://doi.org/10.1130/G23106A.1

Wobus C, Helmsath A, Whipple K, Hodges K (2005) Active out-of-sequence thrust faulting in the central Nepalese Himalaya. Nature 434:1008–1011. https://doi.org/10.1038/nature03499

Zaidi FK (2011) Drainage basin morphometry for identifying zones for artificial recharge: a case study from the Gagas River Basin, India. J Geol Soc India 77:160–166. https://doi.org/10.1007/s12594-011-0019-2

Zhang HP, Zhang PZ, Fan QC (2011) Initiation and recession of the fluvial knickpoints: a case study from the Yalu River-Wangtian'e volcanic region, northeastern China. Sci China Earth Sci 54:1746–1753. https://doi.org/10.1007/s11430-011-4254-6

Zoback ML (1992) First and second-order patterns of stress in the lithosphere: the world stress map project. J Geophys Res 97:11703. https://doi.org/10.1029/92JB00132